Magnetic separation of iron precipitate from nickel sulfate solution by magnetic seeding

Haisheng Han, Wei Sun *, Yuehua Hu, Honghu Tang, Tong Yue

School of Mineral Processing and Bioengineering, Central South University, Changsha 410083, China

ABSTRACT

The application and development of goethite process were hindered by the poor filterability of the precipitate and the great loss of nickel in nickel hydrometallurgy. In this study, the effects of pH on the goethite precipitation and the mechanism of the nickel loss were investigated. The goethite precipitation at a lower pH (2.4 to 3.0) guaranteed a higher recovery of nickel at the cost of the filterability of the precipitate. Then a novel process, magnetic seeding and separation, was proposed to improve the filterability of iron residues and simplify the iron removal process. The iron precipitated on the surface of the magnetic seeds to form a large particle with core-shell structures and the magnetic core endowed the particles magnetism. Efficient magnetic separation offseted the poor settleability and filterability of the precipitate. After magnetic separation of iron residue, the nickel solution was qualified and the dried iron residue contained more than 52% Fe and less than 0.6% Ni, indicating a promising alternative process for treatment of bulky residues of iron precipitate. Further analyses with Environmental scanning electron microscopy (ESEM) and X-ray Diffraction (XRD) provided a fundamental understanding of the new process.

© 2015 Elsevier B.V. All rights reserved.

1. Introduction

Since the early 1970s, various hydrolysis–precipitation methods have been developed for iron removal from hydrometallurgical solution. The widely used techniques, for examples, include the Hematite Process (Ismael and Carvalho, 2003), the Jarosite Process (Claassen et al., 2002; Swarnkar et al., 1996), and the Goethite Process (Davey and Scott, 1976; Pradel et al., 1993). The Goethite Process has the advantages of lower capital expenditure over the Hematite Process and producing eco-friendly products relative to the Jarosite Process. The essential feature of the Goethite Process is that the concentration of ferric iron should be maintained at less than 2 g/L during precipitation (Dutrizac, 1987). This requirement can be met by either reducing all ferric ions to the ferrous state (V.M. method) (Bodson, 1972) or by adding the concentrated pressure leaching solution into a large precipitation vessel at the same rate as goethite precipitation (E.Z. method) (Loan et al., 2006). The E.Z. method led to the development of another two iron removal processes: the Paragoethite Process and Zincor Process (Cubeddu et al., 1996; Meyer et al., 1996). Unlike the Hematite, Jarosite, and Goethite Processes, the Paragoethite and Zincor Processes are much less common, in operation at only three commercial zinc processing sites (Wang et al., 2011). Very little information was available on the exact nature of the Paragoethite and Zincor residues, until recent studies

of Loan et al. (2002) and Claassen et al. (2003) indentified 6-line ferrihydrite and schwertmannite to be the major iron precipitation products.

While the iron removal processes are widely used for solution purification in the zinc industry, their application to nickel sulfate projects has also been explored. Generally, the rejection of iron by precipitation in the hydrometallurgical processing of nickel follows the same routes used in the zinc industry, and an understanding of these processes therefore comes from the studies centered on the processing of zinc. Research has focused on the removal of iron by goethite precipitation from iron-containing nickel sulfate solutions (Allan, 1973; Chang et al., 2010; Wang et al., 2011).

However, several practical problems in iron precipitation as goethite during the nickel hydrometallurgy process are the loss of nickel and the poor filterability of the residues. The recent experimental work on the V.M. process by Chang et al. (2010) has shown that 4.1% nickel was lost with the iron precipitation occurring at pH 2.5 to 3.0, whereas 15.9% was lost for iron precipitation at pH 3.0 to 4.0 in nickel laterite leach solution. Although the exact mechanisms remain unclear, the loss of nickel seems to be related to the parameters affecting the iron precipitation such as pH, temperature, and ratio of iron to nickel in the leach solution. Loss of nickel could be minimized by carefully choosing the right combination of the above parameters (Wang et al., 2011). Wang et al. (2013) confirmed that a "high temperature–low pH, and low temperature–high pH" multi-step neutralizing strategy is best suited to the removal of iron from the nickel laterite leach solutions. However the lower pH or lower temperature often results in the bad filterability of the residues. Claassen et al. (2003) found that the pH

* Corresponding author.
E-mail address: 345340973@qq.com (W. Sun).

Table 1
Composition of nickel sulfate leaching solution.

Analyte	Fe^{2+}	Fe^{3+}	Ni	Cu	Co	S	Na	Pb	Si	As
Content/(g/L)	6.54	0.090	108	0.390	1.38	70.2	10.6	0.110	0.060	0.068

and temperature controlled the particle size and the filtration rate, where lower particle growth and filtration rates were observed at lower pH. And a recent study (Loan et al., 2006) demonstrated that the residues of goethite were amorphous iron phases and 6-line ferrihydrite constitutes around 40–50%. The others were found to be solid-solution jarosite phases, silica, and poorly crystalline goethite. Usually, a more compact residue of increased particle size distribution is often expected to enhance the filtration properties in industrial production. Thus the key point for iron removal is to acquire a compact residue with the less nickel loss under a proper precipitation environment, such as pH, temperature, and supersaturation. This required the development of alternate processing routes such as well-utilized jarosite or efficient goethite process.

This paper proposed a novel process, magnetic seeding and separation, to promote the growth and aggregation of goethite precipitate on the surface of the magnetic seeds, forming a core-shell structure. The magnetic particles will be magnetized and gather together in a magnetic field, accelerating the solid–liquid separation. Combined-analyses were conducted to provide new insights into the mechanism of iron precipitation on the surface of the magnetic seeds.

2. Experimental

2.1. Materials and preparation

Concentrated acidic $NiSO_4$/Fe^{2+} feed liquor that contained 0.1 g L^{-1} H_2SO_4 (pH ≈ 1), 108 g L^{-1} Ni^{2+}, and 6.54 g L^{-1} Fe^{2+} was obtained from the 4th Nickel Smelter of Jinchuan Group Ltd. in Gansu province, China. The nickel smelter adopted the pressure oxidative leaching process. And the components of the materials were analyzed using ICP-AES. As shown in Table 1, the nickel sulfate leaching solution contained a large amount of ferrous ion, as well as a variety of analytes, such as Cd, As, Pb, Cu, Ni, and Mn, accounting for the complication of the nickel-rich solution.

The magnetic seeds were the particles with the core-shell structure. −37 μm magnetite particles served as the core and the goethite precipitates were the shells. And the core-shell structures were prepared by mechanical dry-milling of the mixture of the magnetite and goethite particles for 15–20 min. The qualified magnetic seeds were collected by a magnetic separator with 600 GS magnetic intensity.

2.2. Experimental procedure

The experiments of the effects of pH on goethite process were carried out in a 2-L kettle by the V.M. process. The temperature was maintained at about 85.5 ± 1 °C. The oxidizing agent, hydrogen peroxide, was pumped at a constant rate to generate Fe(III) by oxidation of Fe(II) and the Fe(III) concentration should be kept at low levels (<1 g/L) in the solution. Meanwhile, the neutralizer, sodium carbonate,

Table 2
The effect of pH on the goethite precipitation and the characteristic of the precipitate.

pH	Time for iron precipitation/min	Color of the precipitates	The iron content of the precipitate/%	The filtration time of the precipitate/min
2.0–2.4	60	Black	33.2	30
2.4–2.8	60	Brown	45.6	15
2.8–3.3	60	Brown	51.7	14
3.3–3.8	60	Reddish	54.2	5
3.8–4.5	60	Reddish	55.6	5

was pumped at a flow rate designed to control the pH set point and allowed precipitation to proceed. After the precipitation, the filterability of the residues was measured by a vacuum filter at negative pressure 0.05 MPa.

The experiments of magnetic seeding adopted the optimum parameters with the above-mentioned goethite process. The magnetic seeds were added into the reactor before the precipitation. After the precipitation, polymeric flocculant (10 mg/L) was added to help catch the fine particles for flocculation and the slurry was pumped to the magnetic settling device for magnetic flocculation and rapid solid–liquid separation. Nonionic polyacrylamide (AR grade) served as the flocculant and the molecular weight was 8 million to 14 million.

The residues of the experiments were filtered and the filter cakes were washed with hot sulfuric acid solution (pH 2.5) and dried at 80 ± 5 °C for 2–3 h. After drying, the samples were divided into several portions for a series of analyses.

2.3. Analytical techniques

Different materials were subject to chemical analysis and Inductively Coupled Plasma Atomic Emission Spectrometer (ICP-AES) analyses for mass balance purposes, and X-ray Diffraction (XRD) analysis for characterization of the crystalline phase. Qualitative and semi-quantitative data from Environmental Scanning Electron Microscopy (ESEM) analyses were indicative of the phases and genesis of precipitated particles, thus were used to support the XRD, XRF and chemical analysis findings. Laser particle size analysis (Malvern instruments Ltd., UK) was conducted for providing information on the particle size of the iron precipitate. Specific surface areas were measured by a Micromeritics ASAP2010 nitrogen adsorption instrument (Micromeritics Inc., USA).

3. Results and discussion

3.1. Goethite precipitation at different pHs

3.1.1. Effect of pH on the goethite precipitation
The effect of pH on iron precipitation and characteristics of the precipitate are presented in Table 2. The color, iron grade, and filtration rate

Fig. 1. XRD patterns of goethite precipitate at different pHs.

a. pH 2.0-2.4   b. pH 2.4-2.8   c. pH 2.8-3.3

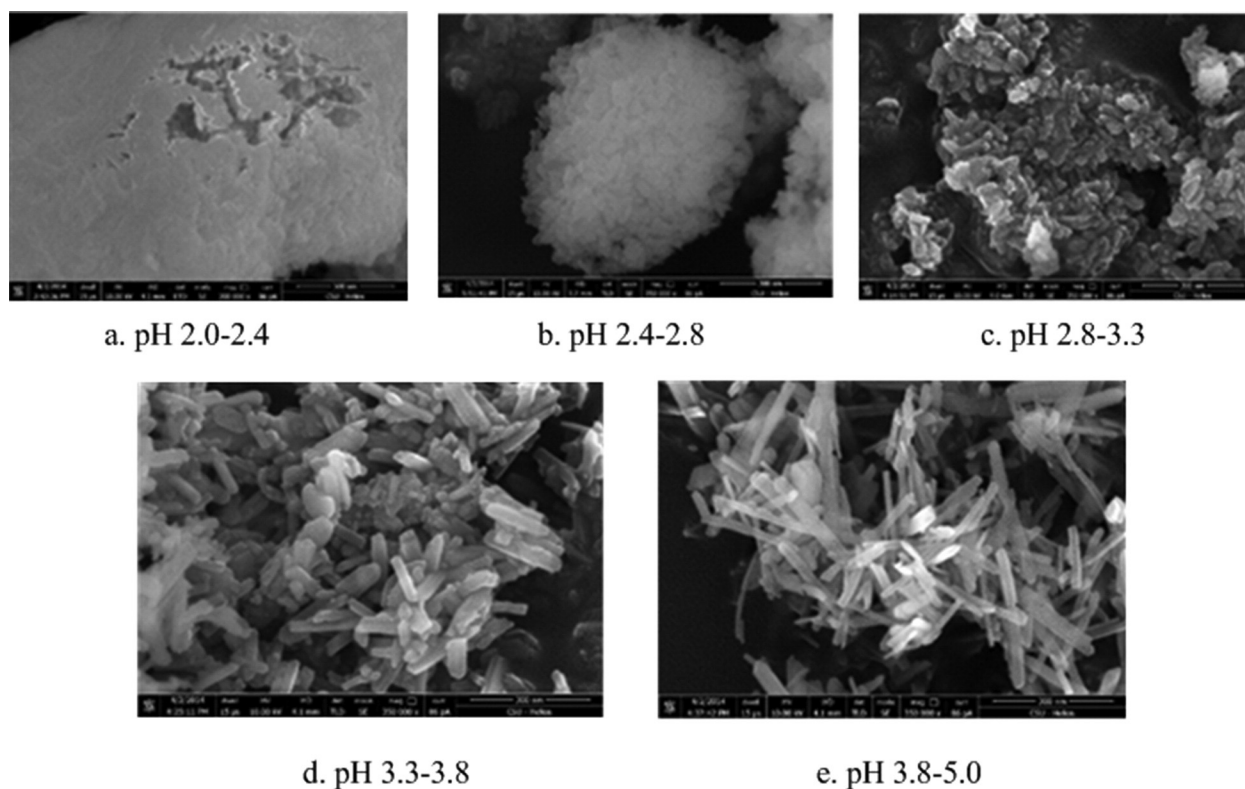d. pH 3.3-3.8   e. pH 3.8-5.0

Fig. 2. SEM images of the goethite precipitate at different pHs.

of the precipitate varied with pH, indicating different features. The black precipitate produced at pH 2.0 to 2.4 contained 43.2% Fe and was difficult to filter. With pH increasing, the filterability of the precipitate was improved and the iron content of that increased.

To provide insight into the effect of pH on the precipitation, XRD patterns and SEM images of the precipitate gained at different pHs are shown in Figs. 1 and 2, respectively. At pH 2.0 to 2.4, the iron precipitate was amorphous and difficult to filter (The last column of Table 2). The XRD patterns of the precipitate demonstrated that most of the iron precipitated as para-goethite at pH 2.4 to 4.5. As the pH increased, the XRD pattern indicated peak narrowing, which implied that the goethite

crystallite size was increasing. This was also confirmed by the SEM images, as shown in Fig. 2(a) to (c). At pH 2.4 to 3.3, the precipitate was poorly crystallized but the fine crystal grain aggregated together to form a big particle. However, the precipitate was needle-like goethite crystallites and had good filterability at higher pH 3.3 to 4.5. The findings were in accordance with the previous work (Wang et al., 2011).

3.1.2. The nickel loss of the goethite process

However the loss of nickel to the precipitate was an important issue during the iron removal process. Fig. 3 demonstrated the recovery of Ni and the crystallinity of the precipitate changed with increasing pH. The
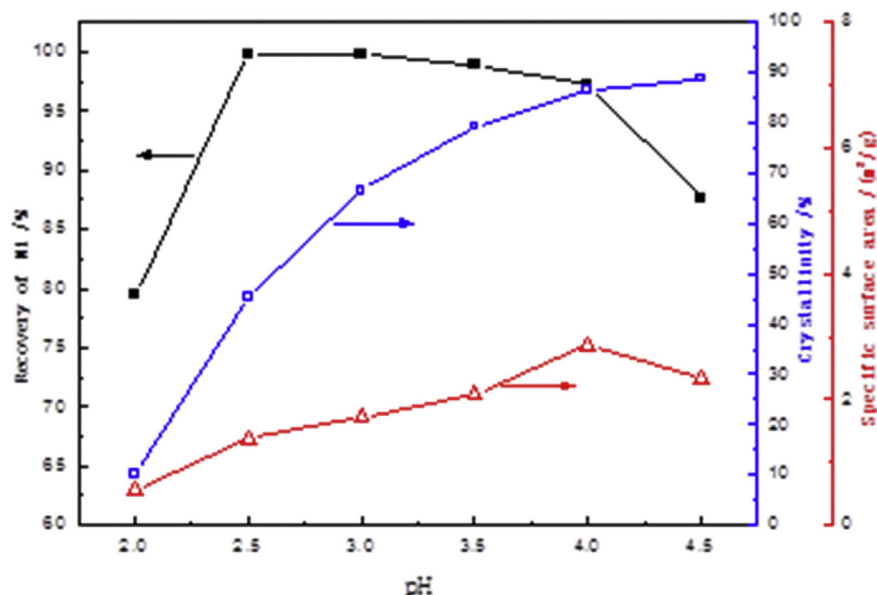

Fig. 3. pH effect for the nickel loss, the crystallinity and the specific surface area of the precipitate.
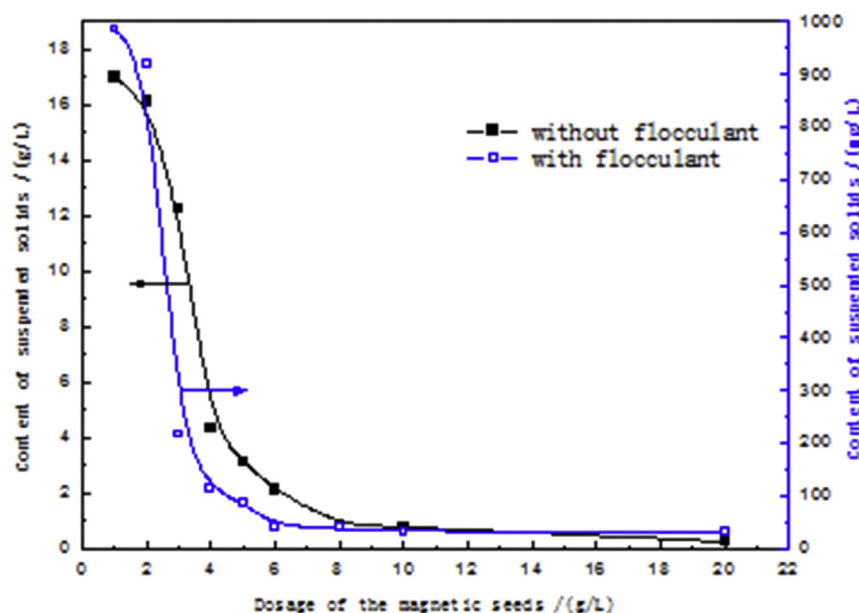
Fig. 4. The effect of dosage of magnetic seeds on iron precipitation (pH 3.0 and temperature 85.5 °C).

pH showed remarkable influence on the nickel loss to the precipitate. When the pH was greater than 3.0 a larger portion of nickel was lost. The loss of nickel in the precipitate may take place by two mechanisms, adsorption or co-precipitation (Carvalho-E-Silva et al., 2003; Singh et al., 2002). Although extensive work have been done, it is still difficult to determine whether the nickel retained by the solids was adsorbed onto the minerals, or precipitated out of solution (Beukes et al., 2000). But it has already been proven that surface area is a determining factor for nickel adsorption on the goethite. Fig. 3 indicated the relationship between the loss of nickel and the specific surface area of the precipitate formed under different pHs. At pH 2.0 to 2.5, although the specific surface area was the smallest, the precipitate was amorphous structure with great loss of nickel. At pH 2.5 to 4.0, the specific surface area of the precipitate and the loss of nickel increased dramatically with the increasing of pH, and adsorption mechanism played a dominant role for the loss of nickel during the iron precipitation. While at pH above 4.0, the loss of nickel was dominated by the co-precipitation mechanism. Although the precipitate was well crystallized and had a relatively smaller specific surface area, the loss of nickel was great. Thus iron precipitation should be conducted at pH 2.5 to 3.5, ensuring the high recovery of nickel.

3.2. Goethite precipitation with magnetic seeds

The precipitation at a lower pH guaranteed a higher recovery of nickel at the cost of bad filterability of the precipitate (the last column of the Table 2). To study the effect of the magnetic seeds on the precipitation, the content of suspended solids of the 10 cm supernatant was tested after magnetic settlement for 10 min. Fig. 4 demonstrated the precipitation was significantly influenced by the dosage of magnetic

seeds. With the increasing of the magnetic seeds, the content of suspended solids decreased dramatically. However the supernatant was still a little turbid even with the addition of large amounts of magnetic seeds, which proved that a small part of fine precipitates did not precipitate on the surface of the seed or aggregate with the magnetic seeds. While the fine nonmagnetic particles aggregated with the magnetic seeds and the turbidity of the supernatant was improved by using the polymeric flocculant and magnetic flocculation. Through this method, the content of suspended solids decreased to 50 mg/L from 1.8 g/L when the dosage of the magnetic seeds was 6 g/L.

Table 3 demonstrated the effect of the addition order of magnetic seeds before or after goethite precipitation on the solid/liquid separation. Without flocculant, the magnetic seeds after precipitation made little contribution to the precipitation and solid/liquid separation. However the magnetic seeds before precipitation significantly contributed to the settling of the precipitate, which proved that goethite was precipitated on the seeds or aggregated with the magnetic particles. With the flocculant increasing, the suspended solids dramatically decreased, but it needed much more flocculant adding magnetic seeds after precipitation. And the supernatant was a little turbid for fine amorphous particles and ferric hydroxide colloid. While the supernatant was much more clear adding magnetic seeds before precipitation for the magnetic seeds promoting goethite precipitation.

Fig. 5 showed the effect of magnetic seeds to the particle size of the residues and indicated that the magnetic seeds significantly contributed to the aggregation of the particles, especially the fine particles (Fig. 5-A). Fig. 5-B indicates that the precipitate with the addition of magnetic seeds had much fewer particles smaller than 1.0 μm than the magnetic seeds, indicating that goethite was precipitated on the seeds or aggregated with the larger particles, resulting in a significant increase in the

Table 3
The effect of the addition order of magnetic seeds before or after goethite precipitation on the solid/liquid separation.

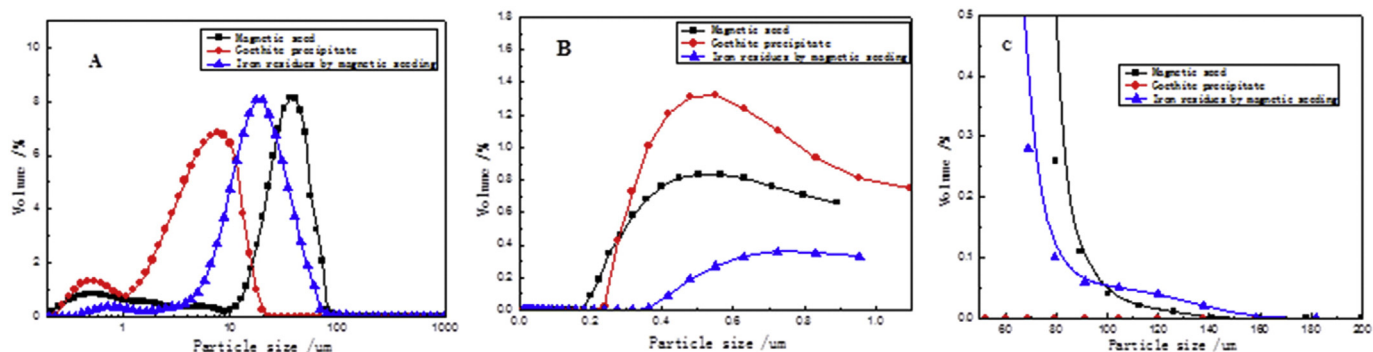| Dosage of flocculant/(mg/L)	Addition order of magnetic seeds	Dosage of magnetic seeds/(g/L)	Content of suspended solids/(g/L)
0	Before precipitation	6	1.8
	After precipitation	6	14.32
10	Before precipitation	6	0.048
	After precipitation	6	3.26
30	Before precipitation	6	0.032
	After precipitation	6	0.258

Fig. 5. The effect of magnetic seeds for the particle size of the residues. (Without flocculant, dosage of magnetic seeds was 6 g · L^{-1}, pH 3.0 and temperature 85.5 °C).

particle size. However the proportion of the large particle of the residue (with the addition of magnetic seeds) was almost smaller than that of magnetic seeds (Fig. 5-C), which proved the fine magnetic seeds played a more significant role for the precipitation. Fig. 6-A and -B were the

SEM analysis of the residues and demonstrated the magnetic seeds were coated with the precipitate forming bigger particles with core-shell structures. The magnetic nucleus endowed the particles magnetism for magnetic separation.
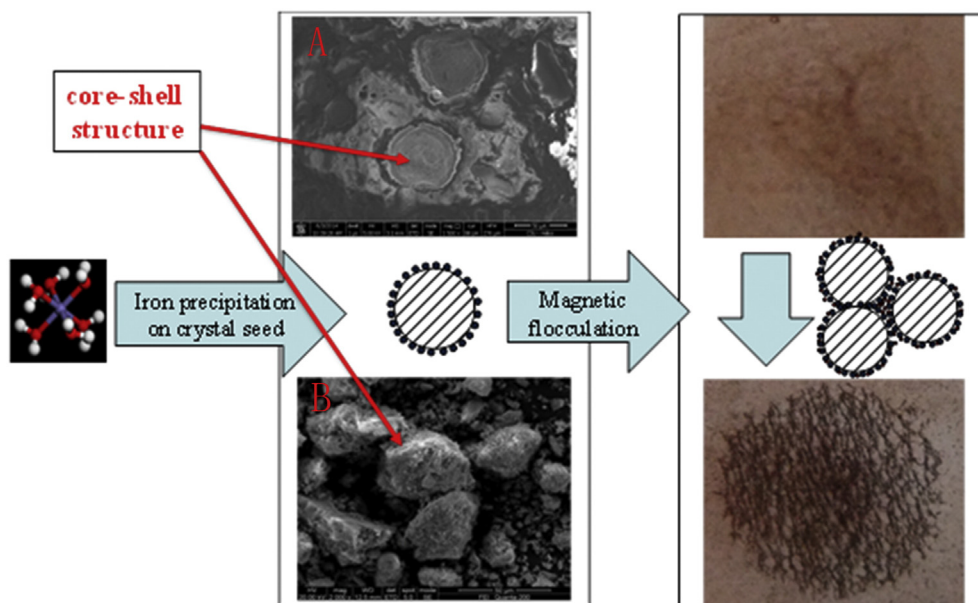

Fig. 6. The process of iron precipitation on the magnetic seeds and the magnetic flocculation in magnetic field. (Fig. 6-A was the surface morphology of the particles and Fig. 6-B showed the core-shell structure of the particles).
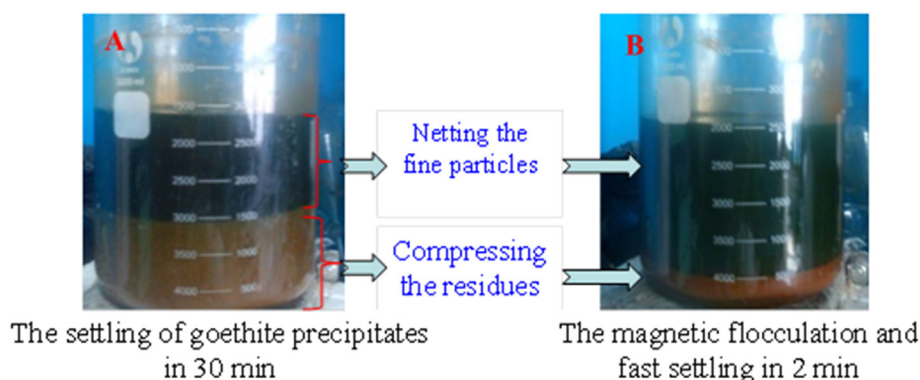

Fig. 7. The sedimentation of the residues by magnetic flocculation or not.

Table 4
The results of magnetic separation for goethite process from nickel leaching solution.

Samples/Elements	Ni	Cu	Fe	Co	S
Leaching solution (g/L)	145	0.062	8.54	1.20	
Qualified liquor (g/L)	124	0.045	0.008	1.20	
Iron residues/%	0.56	0.065	52.89	0.033	1.68
Iron residues after roasting under 600 °C/%	0.73	0.071	63.32	0.035	0.23

3.3. Magnetic flocculation for magnetic particles

Fig. 6 demonstrated the mechanism of the magnetic separation for iron removal. The iron precipitated or aggregated on the surface of the magnetic seeds as goethite, forming a big particle with core-shell structures. And the magnetic core endowed the particle magnetism. For the magnetic particles, pretreatment in a magnetic field could lead to a change of interparticle interaction. By magnetizing the particles apart from van der Waals attraction and electrostatic repulsion, an additional potential is induced, the magnetic attraction, which could easily dominate the other potentials and result in agglomeration in the primary minimum (Stolarski et al., 2007; Yiacoumi et al., 1996). Fig. 7 showed a strong increase of sedimentation velocity by magnetic flocculation of the suspension and proved that magnetic flocculation not only accelerated the settling rate of the particles, but also compressed the residues and enhanced the cake filtration. This lead to a rise in throughput due to the acceleration of sedimentation kinetics.

Table 4 showed the results of magnetic separation for goethite process from nickel leaching solution. The iron residues contained more than 52% Fe and less than 0.6% Ni, which may be suitable for steel production, indicating a promising alternative process for treatment of bulky residues of iron precipitate.

4. Conclusion

In nickel hydrometallurgy, the goethite precipitation at a lower pH guaranteed a higher recovery of nickel at the cost of poor filterability of the precipitates. To solve the filtration problem, magnetic seeding and separation were applied to improve the goethite process. And the experiment proved that the iron precipitated on the surface of the magnetic seeds to form a core-shell structure and the magnetic core endowed the particles magnetism. Then the efficient magnetic flocculation and separation offseted the poor settleability and filterability of the residues. The improved iron precipitation process was not only efficient but also environmentally friendly, and may contribute to the development of the hydrometallurgy process.

Reference

Allan, R.W., 1973. METHOD OF REMOVING DISSOLVED FERRIC IRON FROM IRON-BEARING SOLUTIONS. Google Patents.
Beukes, J.P., Giesekke, E.W., Elliott, W., 2000. Nickel retention by goethite and hematite. Miner. Eng. 13 (14-15), 1573–1579.
Bodson, F.J.J., 1972. RECOVERY OF ZINC VALUES FROM ZINC PLANT RESIDUE. Google Patents.
Carvalho-E-Silva, M.L., Ramos, A.Y., Tolentino, H.C.N., Enweiler, J., Netto, S.M., Alves, M.C.M., 2003. Incorporation of Ni into natural goethite: an investigation by X-ray absorption spectroscopy. Am. Mineral. 88, 876–882.
Chang, Y., Zhai, X., Li, B., Fu, Y., 2010. Removal of iron from acidic leach liquor of lateritic nickel ore by goethite precipitate. Hydrometallurgy 101 (1), 84–87.
Claassen, J., Meyer, E., Rennie, J., Sandenbergh, R., 2002. Iron precipitation from zinc-rich solutions: defining the Zincor Process. Hydrometallurgy 67 (1), 87–108.
Claassen, J., Rennie, J., Van Niekerk, W., Meyer, E., Sandenbergh, R., 2003. Recent developments in iron removal and control at the Zinc Corporation of South Africa. Electrometall. Environ. Hydrometall. 2, 1675–1690.
Cubeddu, F., Piasentin, M., Reilly, F., Meregalli, L., Tolomio, M., 1996. The paragoethite process at the ENIRISORSE–Porto Vesme plant. Iron Control Disposal 147–161.
Davey, P., Scott, T., 1976. Removal of iron from leach liquors by the "goethite" process. Hydrometallurgy 2 (1), 25–33.
Dutrizac, J., 1987. An overview of Iron Precipitation in Hydrometallurgy. CIM BULLETIN. Canadian Inst Mining Metallurgy Petroleum, 101 6TH AVE SW, STE 320, CALGARY AB TZP 3P4, Canada, p. 94-94.
Ismael, M., Carvalho, J., 2003. Iron recovery from sulphate leach liquors in zinc hydrometallurgy. Miner. Eng. 16 (1), 31–39.
Loan, M., Parkinson, G., Newman, M., Farrow, J., 2002. Iron oxy-hydroxide crystallization in a hydrometallurgical residue. J. Cryst. Growth 235 (1), 482–488.
Loan, M., Newman, O., Cooper, R., Farrow, J., Parkinson, G., 2006. Defining the paragoethite process for iron removal in zinc hydrometallurgy. Hydrometallurgy 81 (2), 104–129.
Meyer, E., Howard, G., Haegele, R., Beck, R., 1996. Iron control and removal at the Zinc Corporation of South Africa. Iron Control Disposal 163–182.
Pradel, J., Castillo, S., Traverse, J.P., Grezes-Besset, R., Darcy, M., 1993. Ferric hydroxide oxide from the goethite process: characterization and potential use. Ind. Eng. Chem. Res. 32 (9), 1801–1804.
Singh, B., Sherman, D.M., Gilkes, R.J., Wells, M.A., Mosselmans, J.F.W., 2002. Incorporation of Cr. Mn and Ni into goethite: mechanism from extended X-ray absorption spectroscopy. Clay Miner. 37, 639–649.
Stolarski, M., Eichholz, C., Fuchs, B., Nirschl, H., 2007. Sedimentation acceleration of remanent iron oxide by magnetic flocculation. China Particuol. 5 (1–2), 145–150.
Swarnkar, S., Gupta, B., Sekharan, R.D., 1996. Iron control in zinc plant residue leach solution. Hydrometallurgy 42 (1), 21–26.
Wang, K., Li, J., McDonald, R., Browner, R., 2011. The effect of iron precipitation upon nickel losses from synthetic atmospheric nickel laterite leach solutions: statistical analysis and modelling. Hydrometallurgy 109 (1), 140–152.
Wang, K., Li, J., McDonald, R., Browner, R., 2013. Characterisation of iron-rich precipitates from synthetic atmospheric nickel laterite leach solutions. Miner. Eng. 40, 1–11.
Yiacoumi, S., Rountree, D.A., Tsouris, C., 1996. Mechanism of particle flocculation by magnetic seeding. J. Colloid Interface Sci. 184 (2), 477–488.